

IR Spectra of Water Clusters with Captured Ethane Molecules: Computer Simulation

A. E. Galashev and A. N. Novruzov

*Institute of Industrial Ecology, Ural Division, Russian Academy of Sciences,
ul. Sof'i Kovalevskoi 20a, Yekaterinburg, 620219 Russia
e-mail: galashev@ecko.uran.ru*

Received March 20, 2007

Abstract—Uptake of ethane molecules by a monodisperse aqueous system was simulated by molecular dynamics. The cluster $(\text{H}_2\text{O})_{20}$ characterizing the system remains stable until the number of the captured C_2H_6 molecules becomes larger than four. Addition of ethane molecules to the disperse aqueous system decreases both the real and imaginary parts of the dielectric permittivity in the frequency range $0 \leq \omega \leq 1000 \text{ cm}^{-1}$. The integral IR absorption coefficient of the disperse system containing C_2H_6 molecules increases, and the frequency-average reflection coefficient decreases. The continuous reflection spectra transform into band spectra. The heat-radiating power of the clusters decreases upon absorption of ethane molecules. The cluster that took up two ethane molecules exhibits the highest radiating power. This cluster has the largest number of active electrons interacting with the arriving wave.

DOI: 10.1134/S1070363208010052

It was shown experimentally that ethane has the lowest free energy of hydration among saturated hydrocarbons [1]. Hydration of hydrocarbon molecules is accompanied by a hydrophobic effect caused by rearrangement of the hydrogen bond network in the first solvation layer. The extent of the hydrophobic effect can be evaluated from the solubility of the hydrocarbon. The hydrophobic effect is also observed in dissolution of ethane in water. The hydrogen bonds between two water molecules in the solvation layers of ethane are stronger than in bulk water [2]. Because of the polarizability of molecules, hydrogen bonds enhance each other, i.e., the H bonds between water molecules become stronger owing to the electrostatic induction effect of the solvation layer. The stability of the solvation layer is ensured by attainment of a definite distance between the hydrocarbon molecules in solution. At a certain fixed distance (e.g., 0.48 nm for methane), water molecules form a stable cell accommodating the solute molecules. The stability of the solvation layer is provided by a small number of exchanges between water molecules from the solvation layer and from the bulk.

Absorption of organic molecules by water clusters is still poorly understood. Despite the occurrence of the hydrophobic effect, clusters of water and hydrocarbon molecules can be formed in the gas phase. The results of far-IR studies and DFT calculations are

indicative of the formation of benzene–water dimers [3] and $\text{C}_6\text{H}_6(\text{H}_2\text{O})_9$ clusters [4] in a cooling supersonic beam. The H bond energy in the benzene–water dimer is estimated at $1.9 \text{ kcal mol}^{-1}$. The interaction of the benzene ring with $(\text{H}_2\text{O})_9$ clusters leads to the formation of one H bond and to considerable changes in the distances between the oxygen atoms (and in the distances r_{OH} between O and H atoms of different molecules) in the cluster. The absorption of C_6H_6 molecules should also lead to substantial changes in the structure of the whole water cluster. This, in turn, will appreciably affect the spectral characteristics of the ultradispersed aqueous system, determined by IR spectroscopy. The characteristic frequencies in the absorption spectrum $\alpha(\omega)$ correspond to definite bonds or groups of bonds in a molecule and to a definite steric structure of a molecule. Absorption occurs only when rotation of a molecule leads to changes in the charge distribution in it. In the spectra of the majority of nonpolar molecules, the induced translation and rotation spectra are located in the same frequency range and cannot be observed separately. For liquid water, oscillations with the frequency less than 1000 cm^{-1} correspond to vibration–rotation motion of molecules, whereas the frequencies higher than 1000 cm^{-1} mainly describe intramolecular vibrations [5]. Computer simulation of the interaction of small water clusters with hydrocarbon molecules was made in [6–10]. In [6], we demonstrated the possibility of

uptake of methane molecules by water clusters consisting of 10 and 20 molecules. We found that cluster systems $(\text{CH}_4)_i(\text{H}_2\text{O})_n$ show virtually no IR absorption in a certain frequency range.

The goal of this study was to examine the uptake of ethane molecules by water clusters, reveal the effect of these hydrocarbon molecules on the shape of the IR absorption and reflection spectra of the disperse aqueous system, and elucidate the role of C_2H_6 molecules in the dissipation of the energy of the external IR radiation, taken up by water clusters.

Molecular-dynamic model. Simulation of water clusters was performed with DC model obtained by correction of the Lennard–Jones (LJ) parameters of the TIP4P interaction potential for water and point of location of the negative charge [11]. In so doing, the charges in the H_2O molecule remain unchanged [12]. The geometry of the H_2O molecule corresponds to the experimental parameters of the water molecule in the gas phase: r_{OH} 0.09572 nm, $\angle\text{H–O–H}$ 104.5° [13]. Fixed charges (q_{H} 0.519e, q_{M} –1.038e) are assigned to H atoms and to point M lying on the bisector of the HOH angle at a distance of 0.0215 nm from the oxygen atom. The values of charges and the position of point M were chosen so as to reproduce the experimental dipole and quadrupole moments [14, 15], and also the dimer energy and characteristic distances in the dimer, obtained by ab initio calculations [16]. To point M we assign the polarizability α_i required for calculating the nonadditive polarization energy U_{pol} and induced force f_k^{ind} acting on molecule k [17]:

$$U_{\text{pol}}(\mathbf{R}_{1\dots N}) = -1/2 \sum_i^N \mathbf{E}_i^0 \mathbf{d}_k^{\text{ind}}, \mathbf{d}_k^{\text{ind}} = \alpha_i \mathbf{E}_i, \quad (1)$$

$$f_k^{\text{ind}}(\mathbf{R}_{1\dots N}) = -\nabla_k U_{\text{pol}} = \sum_{i=1}^N \mathbf{d}_i (\nabla_k \mathbf{E}_i^0) + \sum_{i \neq k}^N \nabla_k (\mathbf{d}_i \mathbf{T} \mathbf{d}_k),$$

where \mathbf{R}_i is the radius-vector of point M of the i th molecule; \mathbf{E}_i^0 , Coulomb field strength produced by fixed partial charges; \mathbf{E}_i , field strength in center i , produced both by charges and by interaction of induced dipole moments with these charges; and $\mathbf{d}_k^{\text{ind}}$, induced dipole moment of molecule i .

The dipole tensor is given by the following expression:

$$\mathbf{T}_{ij} = \frac{1}{4\pi\epsilon_v} \frac{1}{r_{ij}^3} \left(\frac{3\mathbf{r}_{ij}\mathbf{r}_{ij}}{r_{ij}^2} - 1 \right),$$

where ϵ_v is the dielectric permittivity of vacuum. To calculate the induced dipole moments, in each time step we used the standard iterative procedure [11]. The accuracy of the determination of \mathbf{d}_i is set in the range 10^{-5} – 10^{-4} D.

The total energy of the interaction between water molecules is given by

$$U_{\text{tot}} = U_{\text{pair}} + U_{\text{pol}}.$$

Here the pair-additive term of the potential is the sum of Lennard–Jones and Coulomb interactions:

$$U_{\text{pair}} = \sum \sum \left\{ 4\epsilon \left[\left(\frac{\sigma_{ij}}{r_{ij}} \right)^{12} - \left(\frac{\sigma_{ij}}{r_{ij}} \right)^6 \right] + \frac{1}{4\pi\epsilon_v} \frac{q_i q_j}{r_{ij}} \right\},$$

where r_{ij} is the distance between points i and j ; q , charge; σ and ϵ , parameters of the LJ potential. The short-range LJ potential with the interaction center assigned to the oxygen atom is responsible for stabilization of the short-range order in water clusters.

The additive term of ethane–water and ethane–ethane interactions was represented in the form of atom–atom functions set through the sum of repulsive, dispersion, and Coulomb contributions:

$$\Phi(r_{ij}) = b_i b_j \exp[-(c_i + c_j)r_{ij}] - a_i a_j r_{ij}^{-6} + \frac{1}{4\pi\epsilon_v} \frac{q_i q_j}{r_{ij}}$$

with the parameters a_i , b_i , and c_i of the potential describing these interactions taken from [18]. To the C and H atoms in the ethane molecule, we assigned the charges $q_{\text{C}}^{\text{ethane}}$ –0.0939e and $q_{\text{H}}^{\text{ethane}}$ 0.0313e, respectively. The polarizability of the C_2H_6 molecule was assigned to its center of gravity (point M). Using the second expression in formula (1), we determined the induced dipole moment of the ethane molecule; its average value was close to the experimental value of 0.3 D [19].

The C_2H_6 molecule has a stable conformation in which rotation around the C–C bond is “braked” [20]. All the H–C–H angles in the ethane molecule are equal, $\sim 109^\circ$, but the group of three H atoms bonded to the second C atom is turned by 60° relative to the group of three H atoms bonded to the first C atom. The following interatomic distances in the C_2H_6 molecule are taken: r_{CC} 0.154 nm, r_{CH} 0.11 nm [19]. Owing to the symmetric distribution of the electric charge in the C_2H_6 molecule, its permanent dipole moment is zero, but the polarizability of the ethane molecule (2.6 \AA^3) is higher than that of the water molecule (1.49 \AA^3) [19].

The trajectories of the centers of gravity of the molecules were determined by the fourth-order Gere method [20]. The time step Δt of the integration was 10^{-17} s, which makes it possible to avoid an increase in the internal energy of the cluster, associated with the accumulation with time of the errors of integration

of motion equations, especially of the equations describing the rotation of molecules. Furthermore, longer time step could lead to destruction of cluster molecules upon introduction of ethane molecules into the region of the action of molecular forces. In the model we used zero or free boundary conditions, i.e., the displacement of molecules was not restricted. Initially in a molecular-dynamics calculation covering the interval $2 \times 10^6 \Delta t$ we prepared an equilibrium state at T 233 K for water clusters containing no impurity molecules. The configuration of the water cluster attained by the time of 20 ps was taken as the initial configuration for simulating the system $(C_2H_6)_i(H_2O)_{20}$. To the water cluster we added no more than six ethane molecules by their initial placement in regions accessible for interatomic interactions. The added C_2H_6 molecules were initially placed so that the shortest distance between the atoms in the ethane molecule and atoms of water molecules was no less than 0.6 nm. The C_2H_6 molecule was arranged so that its C–C axis coincided with the ray connecting the center of gravity of the $(H_2O)_{20}$ cluster with the center of gravity of this molecule. The radius r_c of truncation of all the interactions in the model was 0.9 nm. The quantity r_c is an element of the DC molecule of water. The fitting of the other parameters (values of point charges, geometric characteristics and depth of the potential well) to reproduce the experimental data for water was performed taking into account the truncation of interactions. Therefore, despite the fact that the cluster of 20 water molecules can have a size slightly exceeding r_c , the truncation was preserved. In the case of addition of more than one C_2H_6 molecule to the water clusters, the C–C axes of the added C_2H_6 molecules were arranged on the axes of a rectangular coordinate system with the origin coinciding with the center of gravity of the water cluster. The coordinate axes were “filled” with C_2H_6 molecules in succession, i.e., with two molecules of ethane, they were arranged on the same coordinate axis but on different sides of the center of gravity of the cluster. The newly formed system was equilibrated on the time interval $0.6 \times 10^6 \Delta t$, and then the required physicochemical properties were calculated on the interval $2.5 \times 10^6 \Delta t$. Analytical solution of the motion equations for the rotation of the molecules was done using the Rodrig–Hamilton parameters [21], and the scheme of integration of the motion equations with the occurrence of rotations corresponded to the approach suggested by Sonnenschein [22].

The ultradisperse system consisted of clusters $(C_2H_6)_i(H_2O)_{20}$, i 1, ..., 6. It was assumed that the cluster containing i impurity molecules and 20 water molecules has the following statistical weight:

$$W_i = \frac{N_i}{N_\Sigma}, \quad i = 0, \dots, 6,$$

where N_i is the number of clusters with i impurity molecules and 20 water molecules in 1 cm^3 ; $N_\Sigma = \sum_{i=1}^6 N_i$.

The quantity N was estimated as follows. Consider the scattering of a nonpolarized light in the case when the path length of molecules l is considerably shorter than the light wavelength λ . The extinction (attenuation) coefficient h of the incident beam, on the one hand, is determined by Rayleigh’s formula [23] and, on the other hand, through the scattering coefficient ρ [$h = (16\pi/3)\rho$] [24] in the approximation of scattering at an angle of 90° . Taking into account that $h = \alpha + \rho$, where α is the absorption coefficient, we obtain the following expression:

$$N_i = \frac{2\omega^4 (\sqrt{\epsilon} - 1)^2}{3\pi c^4 \alpha} \left(1 - \frac{3}{16\pi} \right),$$

where c is the velocity of light; ϵ , dielectric permittivity of the medium; and ω , frequency of the incident wave. All the spectrum characteristics were calculated taking into account the assumed statistical weights W_i . The procedure of the formation of cluster systems implies uniform distribution of these formations and is valid at a low concentration of clusters when they do not interact with each other. The mean concentration of each type of clusters in the systems under consideration is 12–13 orders of magnitude lower than the Loschmidt number.

We applied the DC model to the system of 64 water molecules with periodic boundary conditions. The calculated internal energy of liquid water at T 298 K was -0.41 eV , which is in good agreement with the corresponding experimental value (-0.43 eV) [25]. The calculated isothermal compressibility at this temperature is $4.2 \times 10^{-4} \text{ MPa}^{-1}$, and the corresponding experimental value is $4.58 \times 10^{-4} \text{ MPa}^{-1}$ [26].

The calculations were performed with a Pentium IV computer with a CPU frequency of 3.8 GHz. The calculation for cluster $(C_2H_6)_6(H_2O)_{20}$ covering the interval $10^6 \Delta t$ took about 45 h of computer time.

Spectrum characteristics of the clusters $(H_2O)_{20}$ and $(C_2H_6)_i(H_2O)_{20}$. The total dipole moment of the cluster is given by

$$\mathbf{M}(t) = \sum_{i=1}^N \mathbf{d}_i(t),$$

where $\mathbf{d}_i(t)$ is the dipole moment of molecule i and N is the number of molecules in the cluster.

The static dielectric constant ε_0 was calculated through fluctuations of the total dipole moment [27]:

$$\varepsilon_0 = 1 + \frac{4\pi}{3VkT} [\langle \mathbf{M}^2 \rangle - \langle \mathbf{M} \rangle^2].$$

Let us introduce the Fourier–Laplace transform of the function $C(t)$:

$$L_{i\omega}[C] = \int_0^{\infty} dt e^{-i\omega t} C(t).$$

Let us introduce the normalized autocorrelation function \mathbf{M} using the following equality:

$$C(t) = \langle \mathbf{M}(0)\mathbf{M}(t) \rangle / \langle \mathbf{M}^2 \rangle.$$

The frequency dependence of the dielectric permittivity is presented as a complex quantity $\varepsilon(\omega) = \varepsilon'(\omega) - \varepsilon''(\omega)$ with the real part $\varepsilon'(\omega)$ (dielectric dispersion) and imaginary part $\varepsilon''(\omega)$ characterizing the dielectric loss. The correlation between the frequency-dependent dielectric constant and Fourier–Laplace transform of the time derivative of the function $C(t)$ is given by the following relationship [28]:

$$L_{i\omega}[-C] = \frac{\varepsilon(\omega) - 1}{\varepsilon_0 - 1} = 1 - i\omega L_{i\omega}[C].$$

A molecule can absorb electromagnetic waves of a definite frequency only if the dipole moment of the molecule oscillates with the same frequency. The absorption coefficient is proportional to squared amplitude of oscillation of the dipole moment. The radiation absorption at a frequency ω at the thermodynamic equilibrium in the gas phase with a temperature T is characterized by the absorption coefficient α . The quantity α can be represented through the imaginary part of the frequency-dependent dielectric permittivity $\varepsilon(\omega)$ in the following form [29]:

$$\alpha(\omega) = 2 \frac{\omega}{c} \text{Im}[\varepsilon(\omega)]^{1/2}.$$

The reflection coefficient R was determined as the ratio of the mean energy flux reflected from the surface to the incident flux. At normal incidence of a plane monochromatic wave, the reflection coefficient is given by the following formula [23]:

$$R = \left| \frac{\sqrt{\varepsilon_1} - \sqrt{\varepsilon_2}}{\sqrt{\varepsilon_1} + \sqrt{\varepsilon_2}} \right|^2. \quad (2)$$

Here it is assumed that the wave falls from a transparent medium (medium 1) to a medium that can be both transparent and nontransparent, i.e., absorbing

and scattering (medium 2). The indices at the dielectric permittivity in expression (2) denote the corresponding medium.

To calculate the frequency dependence of the dielectric loss $P(\omega)$, we used the following expression [24]:

$$P = \frac{\varepsilon'' \langle E^2 \rangle_{\omega}}{4\pi},$$

where $\langle E^2 \rangle$ is the mean value of the electric intensity squared and ω is the frequency of the emitted electromagnetic wave.

The total number of electrons N_e in unit volume of a cluster interacting with the external electromagnetic field is given by the following relationship [23]:

$$N_e = \frac{m}{2\pi^2 e^2} \int_0^{\infty} \omega \varepsilon''(\omega) d\omega,$$

where e and m are the electron charge and weight.

Stability criterion. The stability to absorption of molecules is characterized by the following criterion [30]:

$$\left(\frac{\partial^2 F}{\partial N^2} \right)_{V,T} > 0,$$

where the free energy differential $dF = -SdT - PdV + \mu dN$, μ is the chemical potential, and N is the number of molecules in the cluster. The excess, relative to ideal gas, free energy of clusters ΔF was calculated by the procedure suggested in [31]. The essence of the quick method for calculating ΔF of a cluster is as follows. The method of thermodynamic perturbation and integration for calculating ΔF is based on variation of the interaction between a given molecule and all the other molecules in the system. The expression for the free energy is as follows:

$$F = kT \ln z, \quad z = \int \exp(-U/kT) dX.$$

The calculation by the perturbation method is performed through the Boltzmann factor weighing the states A and B , at thermal equilibrium of the state A :

$$\begin{aligned} z_B/z_A &= \int \exp(-U_B/kT) dT / \int \exp(-U_A/kT) dX \\ &= \langle \exp(-U_B - U_A/kT) \rangle_A. \end{aligned}$$

For example, B may be a liquid, and A , an ideal gas. For a gradual transition from one state to another, we can perform the integration:

$$\Delta F = \int dF = \int \langle \partial U(\lambda) / \partial \lambda \rangle \partial \lambda,$$

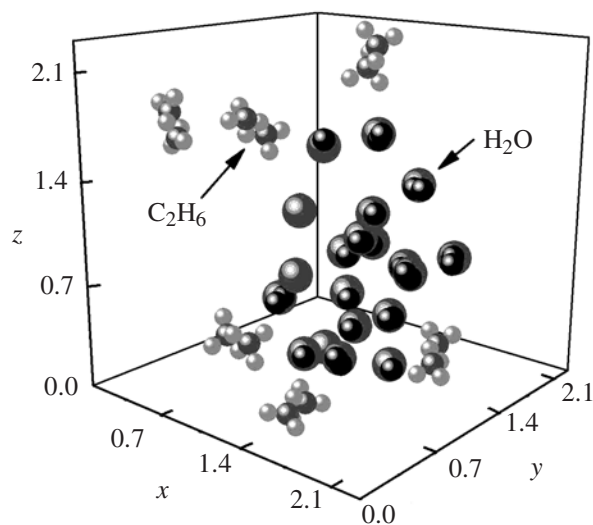


Fig. 1. Configuration of the $(\text{C}_2\text{H}_6)_6(\text{H}_2\text{O})_{20}$ cluster corresponding to the instant of time 25 ps. The molecular coordinates are given in nm.

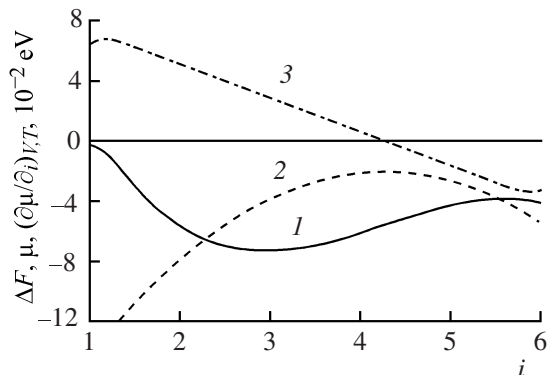


Fig. 2. (1) Excess free energy ΔF , (2) chemical potential μ , and (3) stability coefficient $(\partial\mu/\partial i)_{V,T}$ as functions of the number of C_2H_6 molecules in $(\text{C}_2\text{H}_6)_i(\text{H}_2\text{O})_{20}$ clusters.

where U is a function of parameter λ ; as λ is varied, U varies from U_A to U_B .

The potential energy is determined as the sum of the pair contributions from all the pairs of atoms occurring in different molecules, plus the nonadditive contribution:

$$U = \sum U_{ij} + U_{\text{pol},\lambda},$$

where $U_{\text{pol},\lambda}$ is the polarization energy at the interaction weakened by the λ factor. Our calculation of the excess free energy of water in the polarizable model differs from the calculations for the nonpolarizable model [31] by the presence of an additional term,

$U_{\text{pol},\lambda}$. We also used the functions $f_\alpha(\lambda_\alpha)$ of interaction weakening, as in [31].

Calculation results. The configuration of the $(\text{C}_2\text{H}_6)_6(\text{H}_2\text{O})_{20}$ corresponding to the instant of time 25 ps is shown in Fig. 1. It is seen that no mixing of C_2H_6 molecules with H_2O molecules occurred within this period. Five of six C_2H_6 molecules are in close contact with water molecules of the $(\text{H}_2\text{O})_{20}$ cluster. The sixth C_2H_6 molecule (at upper left) is linked to the cluster through another ethane molecule. The orientation of the C–C axis of the ethane molecules does not correspond to the initial direction and does not have the tangent direction to the aggregate surface as in the case of linear acetylene molecules. One water molecule can form hydrogen bonds with two different ethane molecules, and one ethane molecule can be involved in hydrogen bonds with two water molecules.

Figure 2 shows how the excess free energy ΔF , chemical potential μ , and the derivative $(\partial\mu/\partial i)_{V,T}$ for $(\text{C}_2\text{H}_6)_i(\text{H}_2\text{O})_{20}$ clusters vary with i . It is seen that $\Delta F(i)$ has a minimum, and $\mu(i)$, a maximum near $i = 4$. At $i > 4$ the derivative $(\partial\mu/\partial i)_{V,T}$ becomes negative, suggesting the thermodynamic instability of water clusters that took up more than four ethane molecules.

The frequency dependences of the real and imaginary parts of the dielectric permittivity show that addition of C_2H_6 molecules to water clusters leads to a considerable decrease in these characteristics in the entire frequency range (Fig. 3). For liquid water, ϵ' steeply decreases with increasing frequency. At $\omega > 35 \text{ cm}^{-1}$, ϵ' becomes lower than that for the monodisperse system $(\text{H}_2\text{O})_{20}$, and at $\omega > 250 \text{ cm}^{-1}$ it becomes even lower than that for the system consisting of $(\text{C}_2\text{H}_6)_i(\text{H}_2\text{O})_{20}$ clusters. The function $\epsilon''(\omega)$ for liquid water also decreases with increasing frequency. It undergoes oscillations and then becomes lower than $\epsilon''(\omega)$ for the $(\text{H}_2\text{O})_{20}$ system at $\omega > 260 \text{ cm}^{-1}$ and than $\epsilon''(\omega)$ for the system of $(\text{C}_2\text{H}_6)_i(\text{H}_2\text{O})_{20}$ clusters in a narrow frequency range, $895 \leq \omega \leq 985 \text{ cm}^{-1}$.

From the viewpoint of the greenhouse effect of the disperse system, an important issue is the behavior of the IR absorption coefficient α after addition of impurity molecules to water clusters. In the case of the cluster system $(\text{C}_2\text{H}_6)_i(\text{H}_2\text{O})_{20}$, the dependence $\alpha(\omega)$ becomes smoother than that for the monodisperse system $(\text{H}_2\text{O})_{20}$ (Fig. 4). It is important that, in the frequency range $0 \leq \omega \leq 970 \text{ cm}^{-1}$, the quantity α for the system of clusters containing ethane molecules exceeds that for the $(\text{H}_2\text{O})_{20}$ system. The principal maximum of the function $\alpha(\omega)$ for the $(\text{C}_2\text{H}_6)_i(\text{H}_2\text{O})_{20}$ system is observed at $\omega 973 \text{ cm}^{-1}$, and for the monodisperse system $(\text{H}_2\text{O})_{20}$, at 1036 cm^{-1} . Note that the

experimental spectrum $\alpha(\omega)$ of bulk water has two maxima at ω 200 and 700 cm^{-1} , and the corresponding spectrum of gaseous ethane has a double maximum in the frequency range $810 \leq \omega \leq 840 \text{ cm}^{-1}$.

The frequency dependence of the IR reflection coefficient $R(\omega)$ is continuous with ten peaks for the monodisperse system $(\text{H}_2\text{O})_{20}$, whereas for the $(\text{C}_2\text{H}_6)_i(\text{H}_2\text{O})_{20}$ system actually a band spectrum is observed (Fig. 5), with 19 well-resolved peaks. Furthermore, the mean IR reflection intensity for the $(\text{C}_2\text{H}_6)_i(\text{H}_2\text{O})_{20}$ system is five times lower than that for the $(\text{H}_2\text{O})_{20}$ system.

Clusters that absorbed the IR radiation energy then radiate it into the surrounding space. Uptake of C_2H_6 molecules by $(\text{H}_2\text{O})_{20}$ clusters considerably decreases the emission power P (Fig. 6a). The oscillating spectrum $P(\omega)$ for pure water clusters becomes smooth for the $(\text{C}_2\text{H}_6)_i(\text{H}_2\text{O})_{20}$ system, and the principal maximum for the $P(\omega)$ spectrum shifts from ω 960 cm^{-1} to ω 920 cm^{-1} . The maximal power of the emitted radiation is plotted in Fig. 6b vs. the number i of ethane molecules in the cluster. The function $P_{\max}(i)$ passes through a maximum at $i = 2$, i.e., uptake of two C_2H_6 molecules by the $(\text{H}_2\text{O})_{20}$ cluster gives the largest splash in the $P(\omega)$ function. In other words, addition of two C_2H_6 molecules to the $(\text{H}_2\text{O})_{20}$ cluster leads to the formation of a peculiar emitting dipole. This is also confirmed by Fig. 7 showing how the density N_{e1} of electrons located in the cluster and participating in the interaction with the electromagnetic radiation depends on the number of C_2H_6 molecules taken up by this cluster. The dependence $N_{e1}(i)$ has also a maximum at $i = 2$. Thus, at $i = 2$ the largest number of electrons interacts with the arriving electromagnetic wave, so that specifically the $(\text{C}_2\text{H}_6)_2(\text{H}_2\text{O})_{20}$ clusters absorb the largest energy of the external electromagnetic radiation. This, in turn, leads to the strongest splash (at ω 920 cm^{-1}) of the IR radiation power emitted by this cluster.

The weaker hydrophobicity of ethane, compared to other saturated hydrocarbons, led to closer contact of H_2O molecules of the cluster with absorbed C_2H_6 molecules, compared to CH_4 molecules whose interaction with the water cluster involved merely formation of a shell of methane molecules around the cluster [6]. Examination of the behavior of the function $(\partial m/\partial i)_{V,T}(i)$ shows that the $(\text{H}_2\text{O})_{20}$ cluster remains stable until the number of added C_2H_6 molecules exceeds 4. Addition of ethane molecules to water clusters decreases both the real and imaginary parts of the dielectric permittivity of the ultradisperse system throughout the frequency range $0 \leq \omega \leq 1000 \text{ cm}^{-1}$. The integral IR absorption coefficient of the disperse

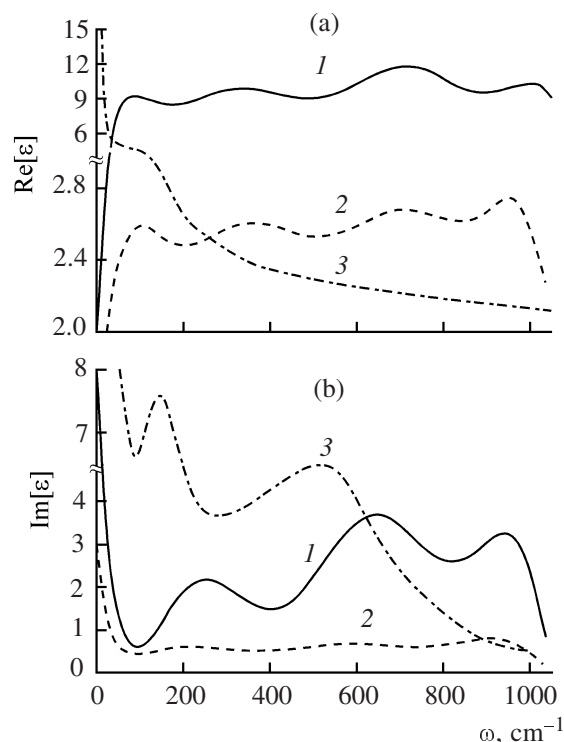


Fig. 3. Frequency dependences of the (a) real and (b) imaginary parts of the dielectric permittivity: (1) monodisperse system $(\text{H}_2\text{O})_{20}$; (2) system of $(\text{C}_2\text{H}_6)_i(\text{H}_2\text{O})_{20}$ clusters, $1 \leq i \leq 6$; (3) (a) molecular-dynamics simulation for liquid water [32] and (b) experimental data for liquid water [33].

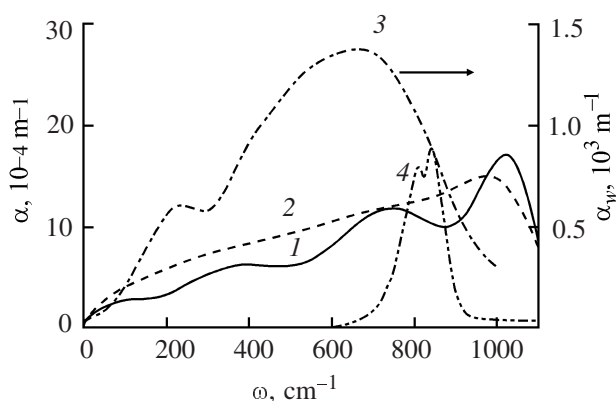


Fig. 4. IR absorption coefficient of cluster systems (1) $(\text{H}_2\text{O})_{20}$ and (2) $(\text{C}_2\text{H}_6)_i(\text{H}_2\text{O})_{20}$; (3) experimental function $\alpha_w(\omega)$ of liquid water [34]; (4) experimental spectrum of gaseous C_2H_6 [35].

aqueous system that took up C_2H_6 molecules somewhat increases relative to that of the monodisperse system $(\text{H}_2\text{O})_{20}$. Absorption of C_2H_6 molecules by the disperse aqueous system leads to a considerable decrease in the frequency-average coefficient of reflec-

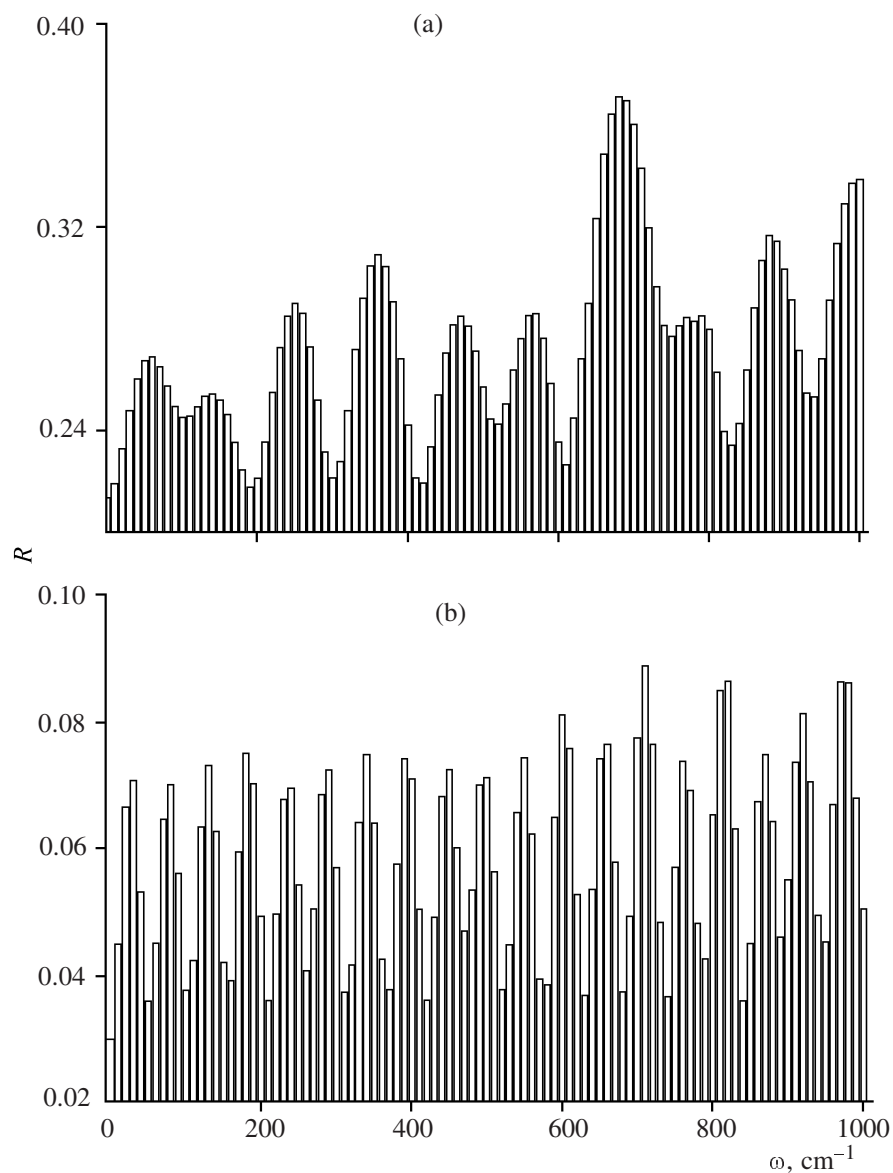


Fig. 5. IR reflection coefficient for cluster systems: (a) $(\text{H}_2\text{O})_{20}$ and (b) $(\text{C}_2\text{H}_6)_i(\text{H}_2\text{O})_{20}$.

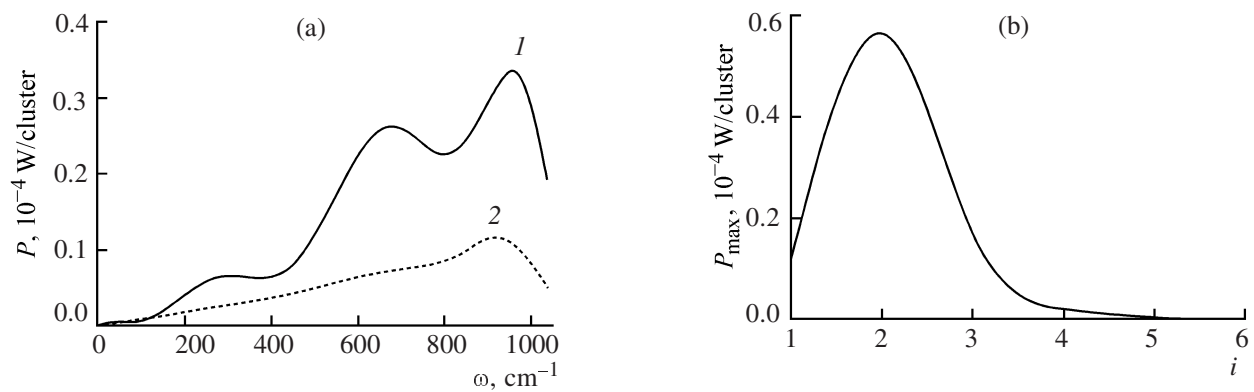


Fig. 6. (a) Frequency dependence $P(\omega)$ of the IR radiation frequency for cluster systems: (1) $(\text{H}_2\text{O})_{20}$ and (2) $(\text{C}_2\text{H}_6)_i(\text{H}_2\text{O})_{20}$; (b) maximal value of P as a function of the number of ethane molecules i in $(\text{C}_2\text{H}_6)_i(\text{H}_2\text{O})_{20}$ clusters.

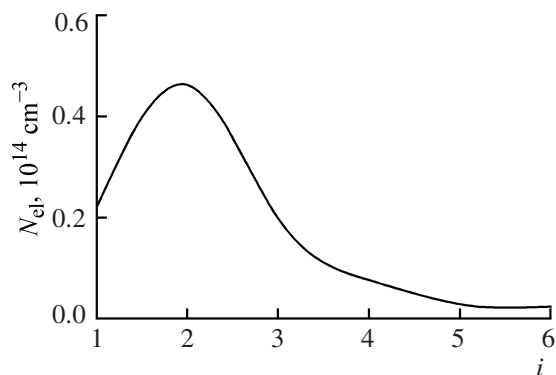


Fig. 7. Density of electrons interacting with the electromagnetic wave in $(\text{C}_2\text{H}_6)_i(\text{H}_2\text{O})_{20}$ clusters.

tion of a plane monochromatic electromagnetic wave, with the continuous reflection spectrum $R(\omega)$ transforming into the band spectrum. The $(\text{H}_2\text{O})_{20}$ clusters that took up ethane molecules and absorbed IR radiation show appreciably decreased integral power of the emitted thermal radiation. Among these clusters, the $(\text{H}_2\text{O})_{20}$ cluster that took up two C_2H_6 molecules shows the maximal IR radiation power. This cluster is also characterized by the maximal number of electrons interacting with the incident electromagnetic radiation.

Thus, we demonstrated a strong dependence of the IR spectra (in particular, reflection and emission spectra) on the presence of ethane molecules in immediate proximity to water clusters. Variation of the character of emission and reflection of electromagnetic waves is determined by physical forces. The interaction between water and ethane molecules causes changes in hydrogen bonding in the clusters. In our model we did not take into account effects related to fluctuation of charges describing the electron density distribution in the molecules. More accurate characteristics of the IR spectra can be obtained with ab initio methods, quick multipole DFT method [36], and method of linear scaling of localized orbitals [37].

ACKNOWLEDGMENTS

The study was financially supported by the Presidium of the Ural Division of the Russian Academy of Sciences (grant for scientific project of young scientists and postgraduate students).

REFERENCES

1. Deshmukh, M.M., Sastry, N.V., and Gadre, S.R., *J. Chem. Phys.*, 2004, vol. 121, no. 24, p. 12402.
2. Xu, H., Stern, H.A., and Berne, B.J., *J. Phys. Chem. B*, 2002, vol. 106, no. 8, p. 2054.

3. Suzuki, S., Green, P.G., Bumgarner, R.E., Dasgupta, S., Goddard, W.A., and Blake, G.A., *Science*, 1992, vol. 257, no. 14, p. 942.
4. Gruenloh, C.J., Carney, J.R., Hagemester, F.C., and Zwier, T.S., *J. Chem. Phys.*, 2000, vol. 113, no. 6, p. 2290.
5. Stern, H.A. and Berne, B.J., *J. Chem. Phys.*, 2001, vol. 115, no. 16, p. 7622.
6. Galashev, A.E., Chukanov, V.N., Novruzov, A.N., and Novruzova, O.A., *Teplofiz. Vys. Temp.*, 2006, vol. 44, no. 3, p. 370.
7. Galashev, A.E., Novruzov, A.N., and Galasheva, O.A., *Khim. Fiz.*, 2006, vol. 25, no. 2, p. 26.
8. Galashev, A.E., Chukanov, V.N., Novruzov, A.N., and Novruzova, O.A., *Elektrokimiya*, 2007, vol. 43, no. 2, p. 143.
9. Galashev, A.Y., Rakhmanova, O.R., Galasheva, O.A., and Novruzov, A.N., *Phase Transitions*, 2006, vol. 79, no. 11, p. 911.
10. Brodskaya, E.N., *Kolloid. Zh.*, 2001, vol. 63, no. 1, p. 10.
11. Dang, L.X. and Chang, T.-M., *J. Chem. Phys.*, 1997, vol. 106, no. 19, p. 8149.
12. Jorgensen, W.L. and Madura, J.D., *J. Am. Chem. Soc.*, 1983, vol. 105, no. 6, p. 1407.
13. Benedict, W.S., Gailar, N., and Plyler, E.K., *J. Chem. Phys.*, 1956, vol. 24, no. 6, p. 1139.
14. Xantheas, S., *J. Chem. Phys.*, 1996, vol. 104, no. 21, p. 8821.
15. Feller, D. and Dixon, D.A., *J. Phys. Chem.*, 1996, vol. 100, no. 8, p. 2993.
16. Smith, D.E. and Dang, L.X., *J. Chem. Phys.*, 1994, vol. 100, no. 5, p. 3757.
17. Ahlstrom, P., Wallqvist, A., Engstrom, S., and Jonsson, B., *Mol. Phys.*, 1989, vol. 68, p. 563.
18. Spackman, M.A., *J. Chem. Phys.*, 1986, vol. 85, no. 11, p. 6579.
19. *Spravochnik khimika* (Chemist's Handbook), Nikol'skii, B.P., Ed., Leningrad: Khimiya, 1971, vol. 1.
20. Morse, J.K., *Physics*, 1928, vol. 14, no. 1, p. 37.
21. Haile, J.M., *Molecular Dynamics Simulation. Elementary Methods*, New York: Wiley, 1992.
22. Koshlyakov, V.N., *Zadachi dinamiki tverdogo tela i prikladnoi teorii giroskopov* (Problems in Solid State Dynamics and Applied Gyroscope Theory), Moscow: Nauka, 1985.
23. Sonnenschein, R., *J. Comp. Phys.*, 1985, vol. 59, no. 3, p. 347.
24. Landau, L.D. and Lifshits, E.M., *Elektrodinamika sploshnykh sred* (Electrodynamics of Continuous Media), Moscow: Nauka, 1982, vol. 8.

25. *Fizicheskaya entsiklopediya* (Physical Encyclopedia), Prokhorov, A.M., Ed., Moscow: Sov. Entsiklopediya, 1988, vol. 1, p. 702.
26. *CRC Handbook of Physics and Chemistry*, Lide, D.R., Ed., London: CRC, 1992, 73rd ed.
27. Bartell, L.S., *J. Phys. Chem. B*, 1997, vol. 101, no. 38, p. 7573.
28. Bresme, F., *J. Chem. Phys.*, 2001, vol. 115, no. 16, p. 7564.
29. Neumann, M., *J. Chem. Phys.*, 1985, vol. 82, no. 12, p. 5663.
30. Shevkunov, S.V., *Kolloidn. Zh.*, 2002, vol. 64, no. 2, p. 262.
31. Hermans, J., Pathiaseril, A., and Anderson, A., *J. Am. Chem. Soc.*, 1988, vol. 110, p. 5982.
32. Neumann, M., *J. Chem. Phys.*, 1986, vol. 85, no. 3, p. 1567.
33. Angell, C.A. and Rodgers, V., *J. Chem. Phys.*, 1984, vol. 80, no. 12, p. 6245.
34. Goggin, P.L. and Carr, C., *Far Infrared Spectroscopy and Aqueous Solutions. Water and Aqueous Solutions*, Bristol: Adam Hilger, 1986, vol. 37, p. 149.
35. Kozintsev, V.I., Belov, M.L., Gorodnichev, V.A., and Fedotov, Yu.V., *Lazernyi optiko-akusticheskii analiz mnogokomponentnykh gazovykh smesei* (Laser Optical-Acoustic Analysis of Multicomponent Gas Mixtures), Moscow: Mosk. Gos. Tekh. Univ., 2003.
36. Kudin, K.N. and Scuseria, G.E., *J. Chem. Phys.*, 1999, vol. 111, no. 6, p. 2351.
37. Schutz, M., Hetzer, G., Werner, H.J., *J. Chem. Phys.*, 1999, vol. 111, no. 13, p. 5691.